Supplement of Nat. Hazards Earth Syst. Sci., 26, 4131–4152, 2026
https://doi.org/10.5194/nhess-26-4131-2026-supplement

Natural Hazards and Earth System Sciences
Open Access

Supplement of

The 2024 cascading glacial lake outburst flood in the Thame Valley of Everest region, Nepal: process, impacts and implications

Nitesh Khadka et al.

Correspondence to: Vishnu Prasad Pandey (vishnu.pandey@pcampus.edu.np)

This file contains

- **Text S1 and S2**
- **Figure S1 to S11**
- **Table S1 to S4**

Text S1. The volumes of water in the lake before and after the GLOF were empirically estimated using nine area-volume relationships (see Table S1). For this, lake area estimated before (2024-08-15) and after (2024-08-18) the event was utilized. The difference in volume between the pre-GLOF and post-GLOF measurements was regarded as the drained volume. The average of all nine estimations was then calculated to determine the overall released volume (Table S1). The standard deviation of the drained volume for each lake was adopted as the volumetric uncertainty. The total uncertainty associated with the cascading GLOF was then computed as the root-sum-square of the individual uncertainties from the upper and lower lakes. The empirically estimated drained volumes were compared with those derived from the post-GLOF DEM.

Notably, the reconstructed drainage volume for the lower lake shows close agreement with the empirical estimates, while drainage volume for the upper lake is underestimated empirically.

Table *Difference between the drained lake volume derived from drone-based DEM and empirical equations in Table S1.*

Lakes	Drone-DEM based (m^3)	Empirical based (m^3)	Differences
Upper	4.10×10^5	$2.5\ (\pm 0.3) \times 10^5$	-64%
Lower	3.60×10^5	$3.5\ (\pm 0.57) \times 10^5$	-2.85%
TOTAL drained volume	7.70×10^5	$6\ (\pm 0.65) \times 10^5$	-28.30%

Text S2 The accuracy assessment of GLOF reconstruction was conducted by comparing the satellite-derived inundation area with the modeled flood extent. True Positive (TP) are the areas flooded in both satellite imagery and model outputs, whereas False Negative (FN) are areas flooded in satellite but not in model (underprediction) and False Positive (FP) are areas flooded in model but not in satellite (overprediction). **Precision** quantifies the reliability of the model's flood predictions, representing the proportion of predicted flooded areas that were actually flooded. **Recall** measures the model's completeness, representing the proportion of actual flooded areas that were correctly captured by the model. **F1 Score** provides a single metric that balances precision and recall by computing their harmonic mean. This is particularly useful when evaluating models where both overprediction and underprediction have important implications, as is the case for GLOF hazard assessment

$$\boldsymbol{Precision} = \frac{TP}{TP+FP} \quad \text{(S1)}$$

$$\boldsymbol{Recall} = \frac{TP}{TP+FN} \quad \text{(S2)}$$

$$\boldsymbol{F1\ Score} = 2 \times \frac{Precision \times Recall}{Precision + Recall} \quad \text{(S3)}$$

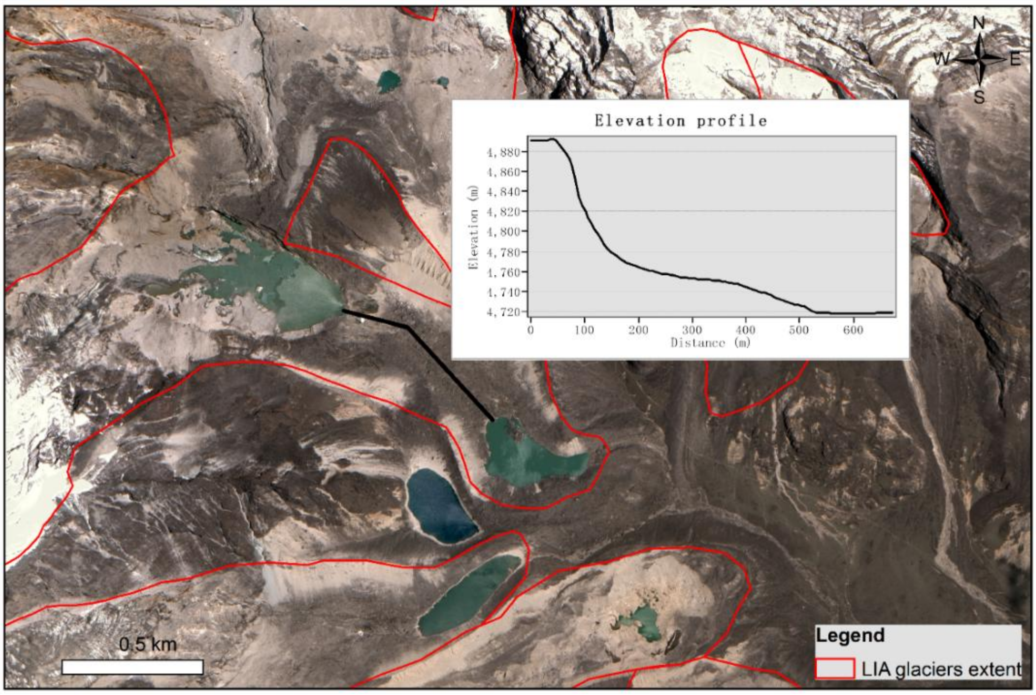

Figure S1 *Elevation profile of flow path connectivity (channel) between upper and lower glacial lakes derived from HMA-DEM along with Little Ice Age (LIA) glacier extent. The LIA glacier outlines were obtained from Lee et al. (2021). The background is from Gaofen image of 2024-5-30. The figure was created by authors using ArcGIS® software by Esri. HMA-DEM courtesy of NASA and USGS. Gaofen satellite imagery courtesy of CNSA and CAST.*

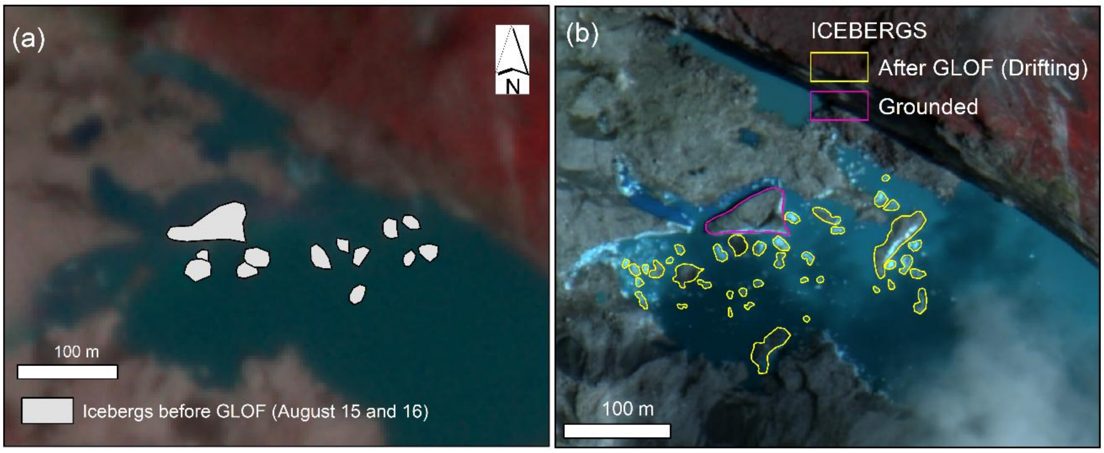

Figure S2 *The icebergs delineated before the GLOF event from PlanetScope images of 2024 August 15 and 16 (a) and from Gaofen image of 2024-8-18 after its outburst (b). The figure was created by authors using ArcGIS® software by Esri. We distinguished drifting and grounded icebergs by comparing their positions in sequential satellite images in ArcGIS. Drifting icebergs exhibited measurable displacement between image acquisitions, whereas grounded icebergs remained stationary. A grounded iceberg is still an iceberg and remains largely buoyant; however, its submerged keel is in contact with the lake bed, temporarily anchoring it and preventing movement. PlanetScope imagery courtesy of Planet Labs PBC. Gaofen satellite imagery courtesy of CNSA and CAST.*

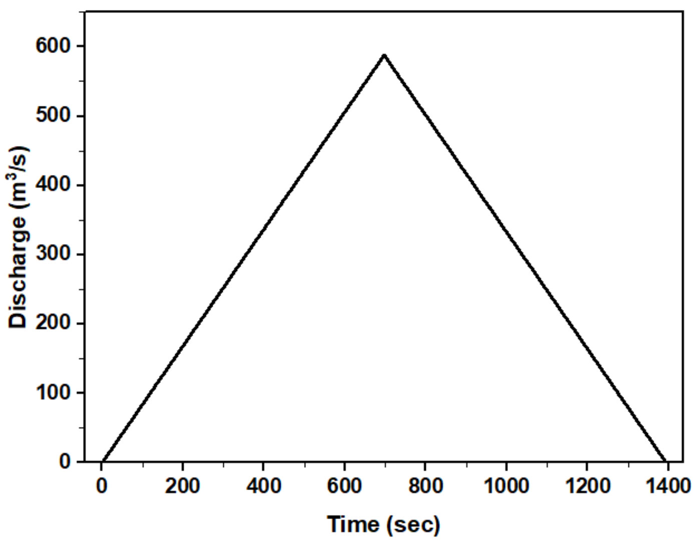

Figure S3 *Inflow discharge at upstream input 1 for Scenario A.*

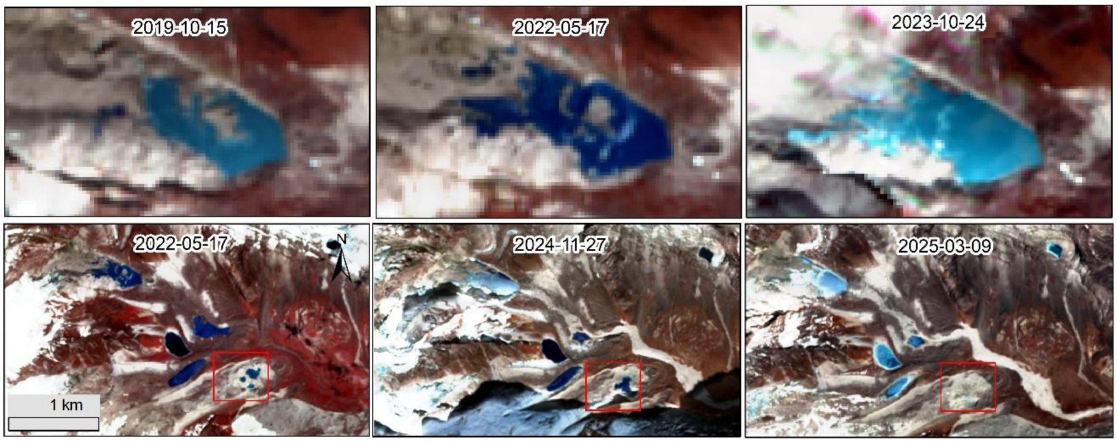

Figure S4 *The rapid expansion of upper lake between 2019 and 2023 (upper panel) and ephemeral nature of lake 5 (red box) shown by Sentinel-2 timeseries images. The figure was created by authors using ArcGIS® software by Esri. Copernicus Sentinel data courtesy of the European Commission and ESA.*

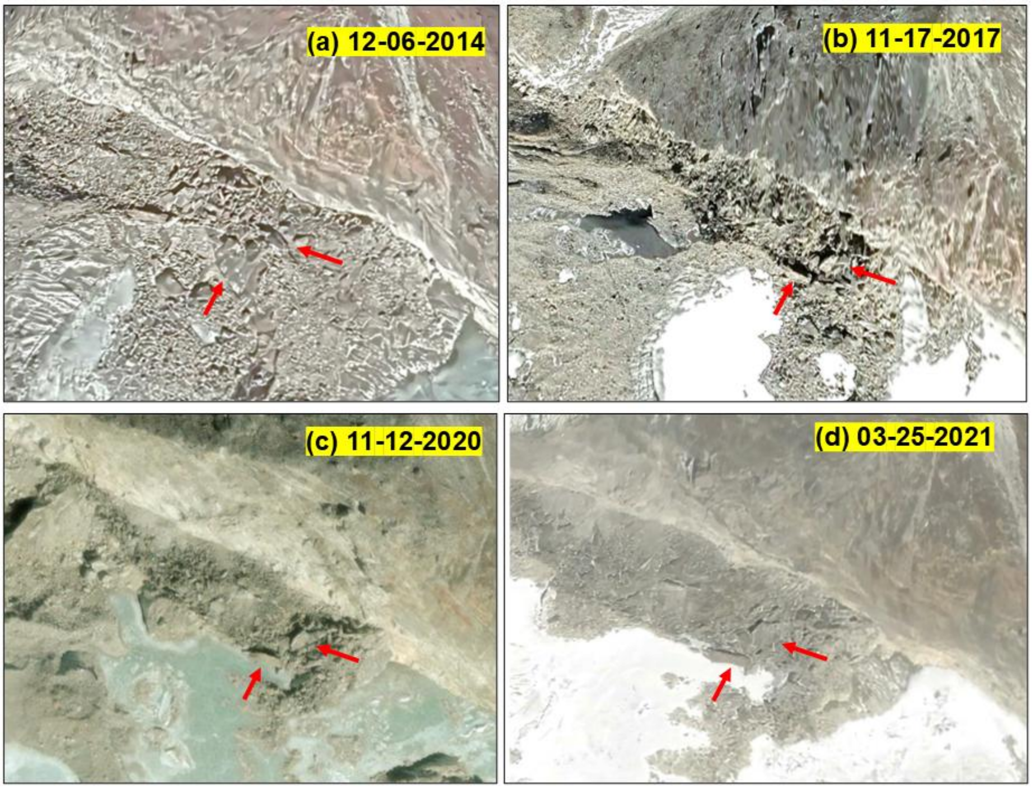

Figure S5 *The time series satellite images showing the deposition of rockfalls pre-GLOF from 2014 to 2021. The images in a, b and d are from © Google Earth collection; images: © CNES/Airbus, Maxar Technologies, Airbus CNES/Airbus and c is from ESRI (Sources: Esri, TomTom, FAO, USGS | Powered by Esri).*

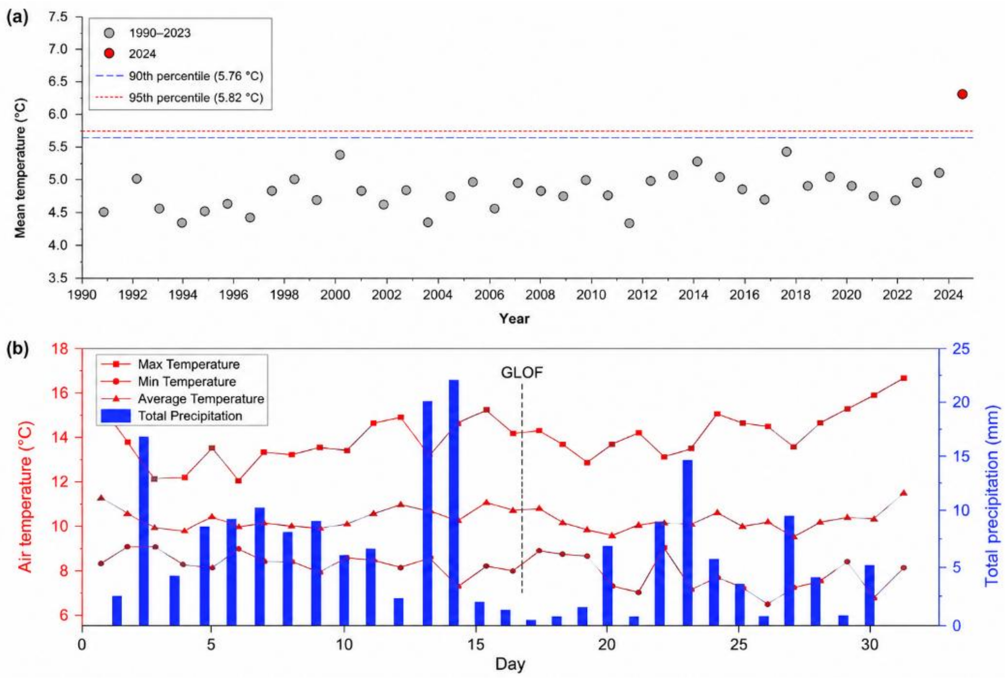

Figure S6 *(a) Mean air temperature during the 30-day pre-event period (17 July–15 August) for 1990–2024. The 2024 pre-event period was the warmest in the available record and exceeded both the 90th and 95th percentile thresholds derived from the same period. (b) Daily air temperature (maximum, minimum, and mean) and precipitation during August, showing anomalously warm and wet conditions preceding the GLOF obtained from Phortse Automatic Weather Station.*

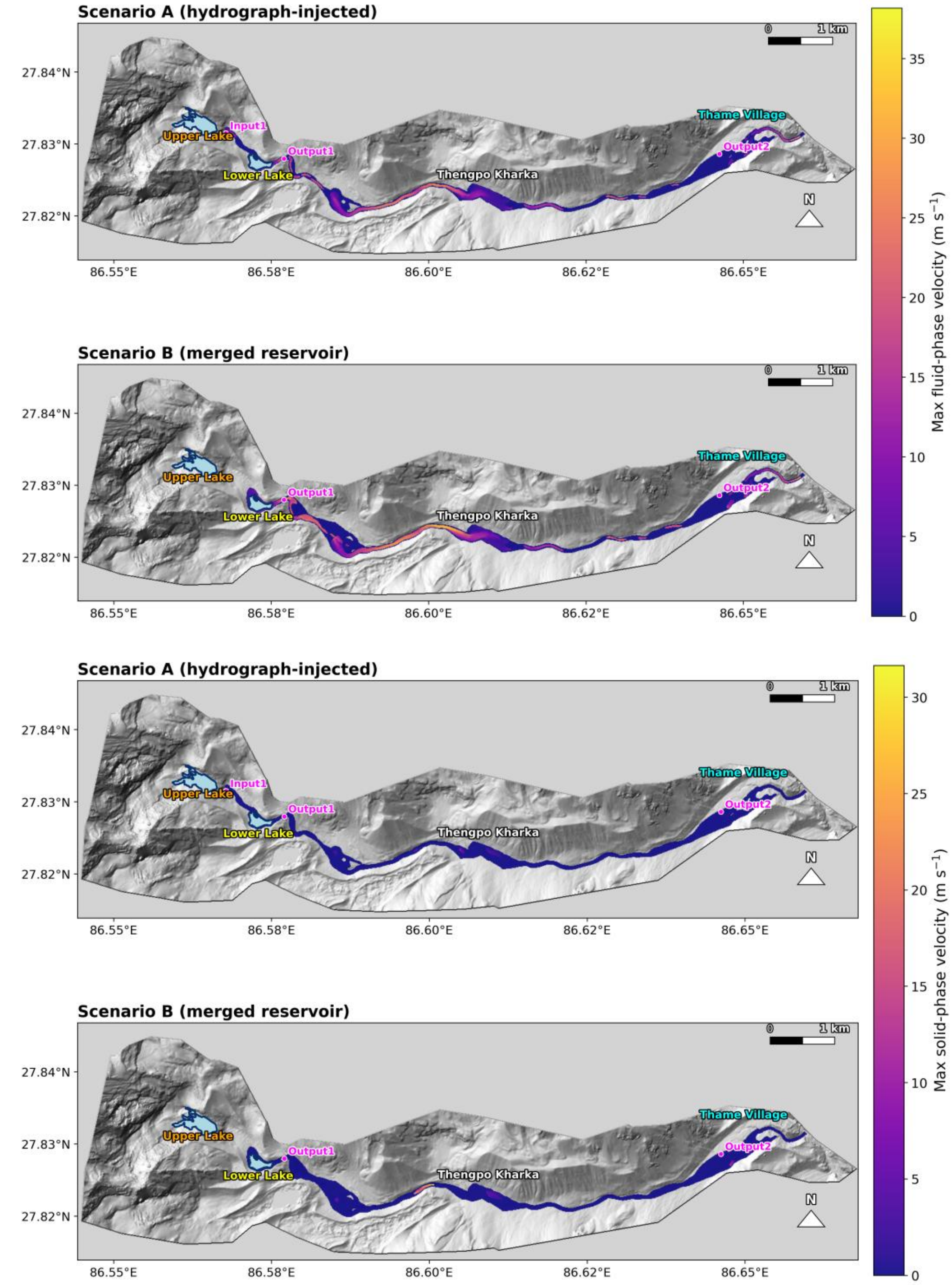

Figure S7 *Simulation results of max velocity maps (upper: fluid phase and lower: solid phase) for scenarios A and B. The background is hillshade of HMA DEM. HMA-DEM courtesy of NASA and USGS.*

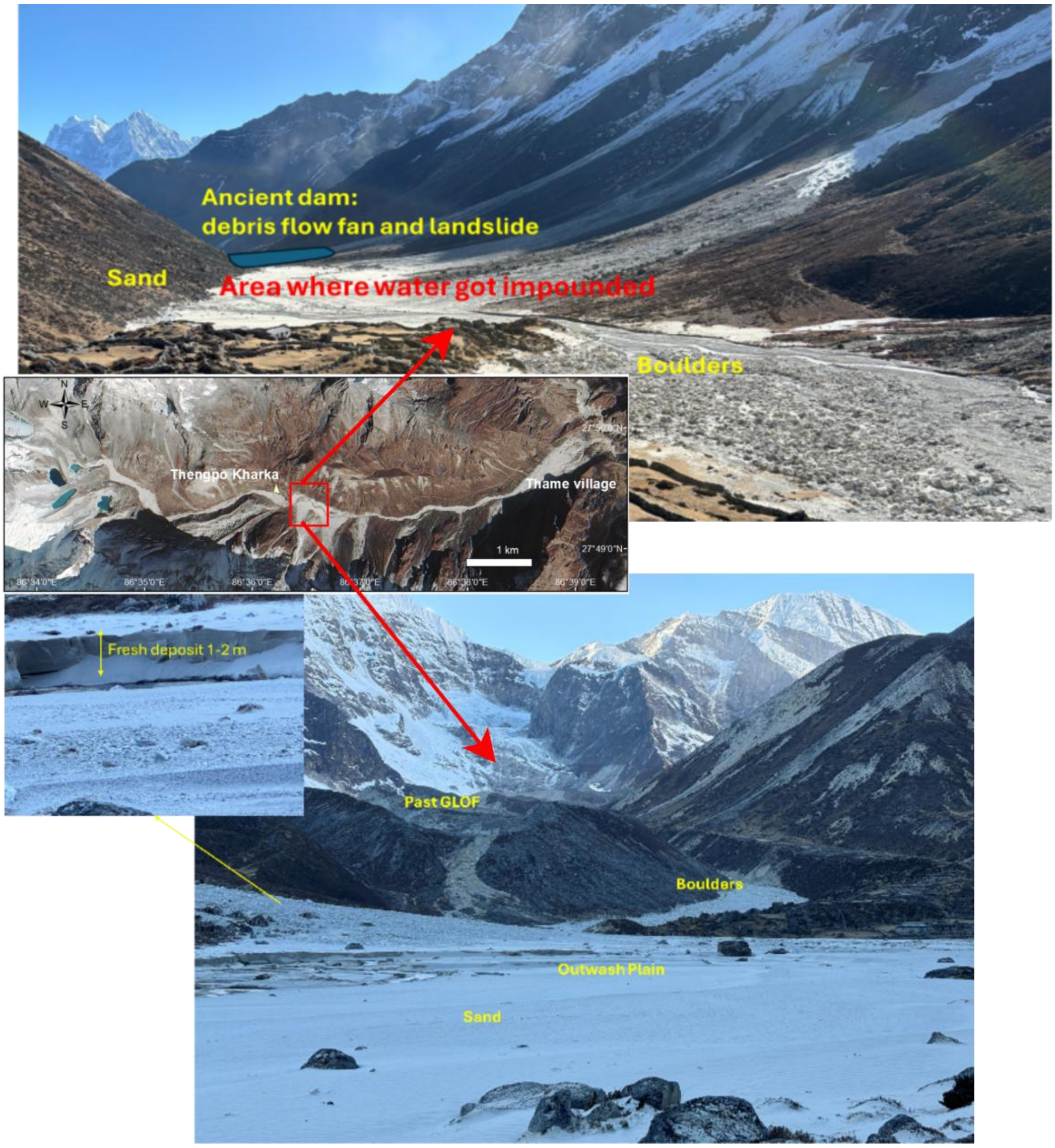

Figure S8 *The ancient debris flow and landslide dam downstream of Thengpo Kharka Village where GLOF water was temporarily impounded. The base image of inset map is from Gaofen satellite. Gaofen satellite imagery courtesy of CNSA and CAST. Photo by K. Sharma, 2024.*

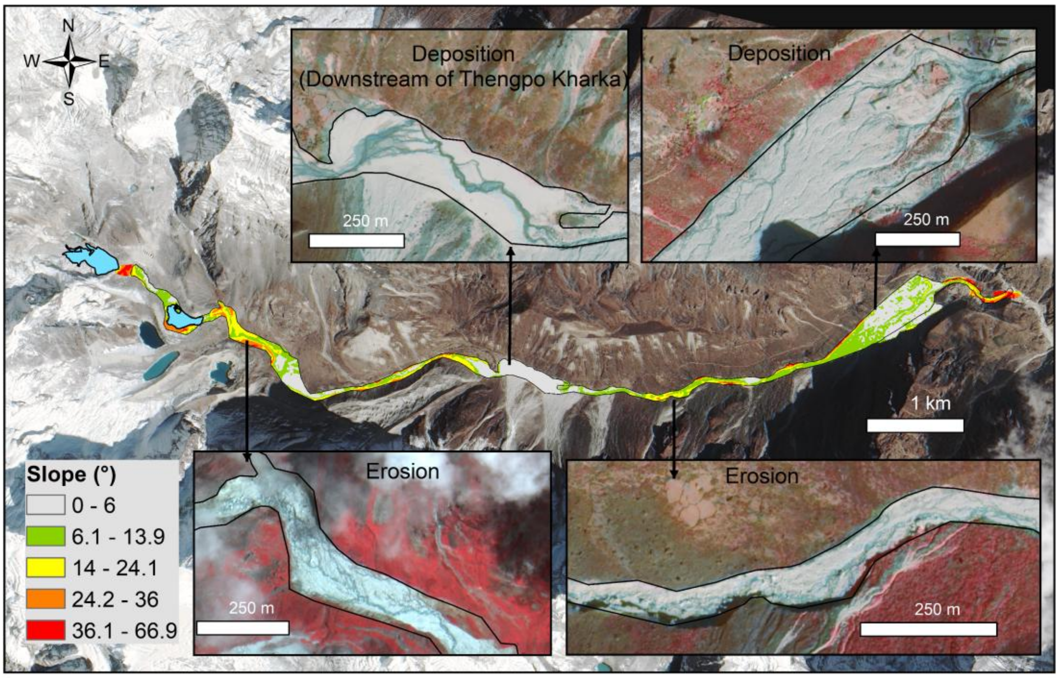

Figure S9 *The erosion and deposition zones along the river channel due to the GLOF event. The base map is from Gaofen image of August 18, 2024. Gaofen satellite imagery courtesy of CNSA and CAST. The figure was created by authors using ArcGIS® software by Esri.*

Figure S10 *Ongoing channel erosion and debris deposition along the Thame stream in Thame Valley, Nepal, showing the close interaction between active geomorphic processes and nearby settlements and infrastructure. Photo by N. Khadka, 2024.*

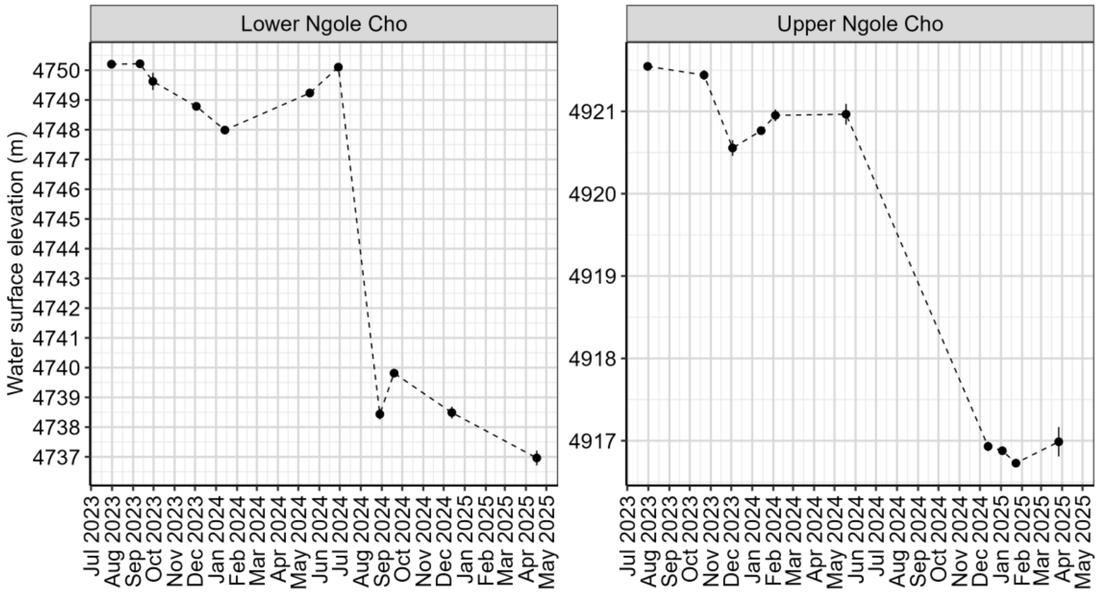

Figure S11 *Time series of water surface elevation for the lower and upper Ngole glacial lakes derived from Surface Water and Ocean Topography (SWOT) data. Courtesy: NASA/CNES SWOT mission via PO.DAAC/AVISO+.*

Table S1 *The volume of glacial lakes before and after their outburst estimated from empirical equations. The lake area and volume are in m^2 and m^3 unless otherwise stated.*

Equation	**Description**	**Volume before outburst**		**Volume after outburst**		**Difference**		Reference
		Upper lake	**Lower lake**	**Upper lake**	**Lower lake**	**Upper**	**Lower**	
$V=0.035A^{1.5}$	A= lake area	1276900.54	368069.56	1057366.74	70835.02	219533.80	297234.54	Evans (1986)
$V=0.104A^{1.42}$	A= lake area	1499032.17	461738.3	1253860.44	97025.01	245171.73	364713.29	Huggel et al. (2002)
$V=A\cdot D$, where $D=0.087A^{0.434}$	A= lake area; D=depth (m)	1475286.48	449178.74	1231827.57	92945.27	243458.91	356233.47	Wang et al. (2012)
$V=43.24A^{1.5307}$	A in km^2 and V in 10^6 m^3	1474299	414287.5	1216122.6	77085.43	258176.40	337202.07	Sakai (2012)
$V=0.0578A^{1.4683}$	A= lake area	1459502.08	431911.09	1213402.19	86067.11	246099.89	345843.98	Khanal et al. (2015)
$V=0.1217A^{1.4129}$	revised fit of Huggel et al. (2002)	1615378.52	500514.11	1352385	105996.5	262993.52	394517.61	Cook and Quincey (2015)
$V=0.036A^{1.49}$	A= lake area	1169439.08	339900.62	969599.5	66136.51	199839.58	273764.11	Kapitsa et al. (2017)
$V=42.95A^{1.408}$	A in km^2 and V in 10^6 m^3	1919747.3	597242.68	1608191.5	127164.00	311555.80	470078.68	Zhang et al. (2023a)
$V=48.58A^{1.59}$	For periglacial lake (lower lake)		388714.81		67765.44		320949.37	Zhang et al. (2023b)
$V=44.47A^{1.5}$	For proglacial lake (upper lake)	1622393.35		1343459.97		278933.38		
Average		1501330.95	439061.9	1249579.50	87891.14	251751.44	351170.8	
Volume released (m^3)						**~2.5*10^5**	**~3.5*10^5**	

Table S2 *Estimation of peak discharge and breach time from different empirical equations. The Q_p, V_G, B_d and T_b are in m^3/s, m^3, m and seconds, unless otherwise stated. Here, breach depth (B_d) is lake level change after GLOF, which is 4.6 and 12 m for upper and lower lake, respectively and for cascading the lower lake breach depth is considered. The volume released utilized from drone-derived DEM.*

Equation	**Description**	**Upper lake**	**Lower lake**	**Upper + lower released volume (cascading)**	**Source**
Peak discharge (Q_p)					
$Q_p=0.72V_G^{0.53}$	V_G= volume released	679.38	634.13	948.8	Evans (1986)
$Qp=0.0048V_G^{0.896}$	V_G= volume released	513.22	456.77	902.69	Popov (1991)
$Q_p = 136\cdot(B_d\cdot V_G)^{0.73}$	V_G= volume released in Mm^3 B_d= breach depth (lake level change)	216.12	395.77	689.42	COSTA and SCHUSTER (1988)
$Q_p=1.122V_G^{0.57}$	V_G= volume	1775.34	1648.49	2542.69	Costa (1985)
$Q_p=0.981(V_G\cdot B_d)^{0.42}$	V_G= volume	424.03	600.59	826.52	Costa (1985)
$Q_p= 0.607(B_d^{1.24}\cdot V_G^{0.295})$	V_G= volume B_d= breach depth	182.30	576.08	720.93	Froehlich (1995)
$Q_p=142\cdot B_d^{0.766}\cdot V_G^{0.378}$	V_G= volume released in Mm^3 B_d= breach depth	326.29	647.48	863.05	Froehlich (2025)
Average		**588.10**	**708.47**	**1070.59**	
Breach Time (T_b)					
$T_b=0.00254(V_G)^{0.53}\cdot B_d^{-0.9}$	V_G= volume released B_d= breach depth	2184.90	860.43	1287.4	Froehlich (1995)
$T_b= [V_G^{0.622}/(71\cdot B_d^{0.766})]\cdot 10^6$	V_G= volume released in Mm^3 B_d= breach depth	2513.17	1112.02	1784.38	Froehlich (2025)
Average		**2349.03**	**986.22**	**1535.89**	

Table S3 *The areas of Lakes 3, 4 and 5 in different time delineated from satellite images.*

Date	**Lake No**	**Area (km^2)**	**Error (km^2)**	**Perimeter (km)**
1976-11-13	3	0.052	0.026	0.88
1989-11-09	3	0.055	0.014	0.96
1995-10-09	3	0.055	0.014	0.91
2000-11-23	3	0.057	0.014	0.93
2005-11-10	3	0.056	0.014	0.93
2009-10-05	3	0.057	0.014	0.93
2015-11-17	3	0.057	0.014	0.93
2020-10-09	3	0.053	0.004	0.90
2024-5-30	3	0.042	0.001	0.81
1976-11-13	4	0.063	0.030	0.98
1989-11-09	4	0.067	0.016	1.08
1995-10-09	4	0.073	0.017	1.12
2000-11-23	4	0.068	0.016	1.10
2005-11-10	4	0.068	0.017	1.11
2009-10-05	4	0.066	0.016	1.10
2015-11-17	4	0.067	0.016	1.08
2020-10-09	4	0.055	0.005	1.06
2024-5-30	4	0.042	0.001	0.99
2020-10-09	5	0.048	0.005	0.93
2024-05-17	5	0.021	0.005	0.93
2024-11-27	5	0.027	0.004	0.83
2024-5-30	5	0.011	0.001	0.70
2025-9-3	5	0.006	0.001	0.40

Table S4 *GLOF susceptibility assessment of upper and lower lakes (GAPHAZ, 2017). An expert assessment of high (***), moderate (**), and low (*) susceptibility for each of the factors is indicated. Factors not considered relevant for these lakes are indicated with –.*

Susceptibility factors for GLOFs	**Relevance**			**Key Attributes**	**Susceptibility of each lake**		**Assessment methods and/or data**
	Con.	**Trig.**	**Mag.**		**Upper lake**	**Lower lake**	
1. Atmospheric factor							
Temperature	+	+		Mean temperature	*Increasing* ***	*Increasing* ***	ERA5-Land data analysis
	+	+		Intensity and frequency of extreme temperature	*Evident* ***	*Evident* ***	
Precipitation		+	+	Intensity and frequency of extreme precipitation	*Evident* ***	*Evident* ***	
2. Cryospheric factor							
Permafrost conditions	+	+	+	State of permafrost, distribution and persistence within lake dam area and bedrock surrounding slopes	*The presence of permafrost in the dam and the surrounding slope is not evident and is located above 5000 m* *	*The presence of permafrost in the dam and the surrounding slope is not evident* -	Google Earth imagery and (Singh et al., 2025)
Glacier retreat and down wasting	+		+	Enlargement of proglacial lakes, enhanced supraglacial lake formation, dam removal or subsidence.	*Glaciers in the catchment are shrinking and lake has capacity to expand upwards due to glacier calving* ***	*No capacity to expand* *	Ice thickness data and this study
Ice avalanche potential		+	+	Steep glacier tongue or ice cliffs, crevasse density and orientation, ice geometry	*Has potential ice avalanche area from the western northern zone* ***	*None* -	This study and trajectory study (Dubey et al., 2023)
Advancing glacier (incl. surging)	+			Formation of ice-dammed lakes	*Not relevant* -	*Not relevant* -	Google Earth
Glacier flow regime	+			Glacier flow velocity	*Relevant* *	*Not relevant: no glacier* -	(Gardner et al., 2019)
Calving potential		+	+	Width of glacier calving front, activity, crevasse density	*Wide Calving front and actively calving* ***	*Glacier not in contact with lake* -	This study
Lake size	+		+	Area, volume, and/or depth	*Volume: 1249579.50* m^3 **	*Volume: 87891.14* m^3 *	This study
3. Geotechnical and geomorphic							
Dam type	+		+	Bedrock, moraine, ice	*Bed rock* *	*Moraine* **	Field study
Ice cored moraine	+			Presence of buried ice	*No* -	*No* -	Field study
Downstream slope of dam	+			Steep Lakefront Area angle greater than 10°	*Yes* *	*No* -	Google Earth

Vegetation on dam	+			Density and type of vegetation (grass, shrubs, trees)	*None -*	*None -*	Field photo and Google Earth imagery
Catchment area	+			Total size of drainage area upstream of catchment	*5 km^2 **	*9 km^2 ***	DEM and GIS-based modelling
Catchment drainage density	+			Density of the stream network in the catchment area	*Higher than lower lake **	*Low **	DEM, GIS-based modelling
Catchment stream order	+			Presence of large fluvial stream facilitating rapid drainage into lake	*Medium order **	*High order **	DEM, GIS-based modelling
Upstream lake		+	+	Presence and susceptibility of upstream lakes	*No lakes -*	*One lake ****	Satellite image
Rock avalanche potential		+	+	Steep, structurally unstable bedrock slopes with potential to runout into the lakes	*Has a large topographic potential of rockfall or rockslides ****	*None -*	DEM, GIS-based topographic assessment and runout modelling (Dubey et al., 2023)
Side moraine instabilities		+	+	Potential for landslides from moraine slopes into the lake	*Insignificant because of lateral bedrock banks -*	*Possible, but the gradient is low **	Field observation and Google Earth
Seismicity		+		Peak ground acceleration *(It has no influence on bedrock dam unless it triggers slope movements)*	*High ****	*High ****	PGA Seismic maps (Rahman and Bai, 2018)

References:

Cook, S. and Quincey, D.: Estimating the volume of Alpine glacial lakes, Earth Surface Dynamics, 3, 559, https://doi.org/10.5194/esurf-3-559-2015, 2015.

Costa, J. E.: Floods from dam failures, 560, US Geological Survey1985.

COSTA, J. E. and SCHUSTER, R. L.: The formation and failure of natural dams, GSA Bulletin, 100, 1054-1068, 10.1130/0016-7606(1988)100<1054:TFAFON>2.3.CO;2 %J GSA Bulletin, 1988.

Dubey, S., Sattar, A., Goyal, M. K., Allen, S., Frey, H., Haritashya, U. K., and Huggel, C.: Mass Movement Hazard and Exposure in the Himalaya, 11, e2022EF003253, https://doi.org/10.1029/2022EF003253, 2023.

Evans, S. G.: The maximum discharge of outburst floods caused by the breaching of man-made and natural dams, Canadian Geotechnical Journal, 23, 385-387, 10.1139/t86-053, 1986.

Froehlich, D.: Predicting Peak Discharge of Outburst Floods from Moraine-Dammed Glacial Lakes, Natural Hazards Review, 26, 04025047, https://doi.org/10.1061/NHREFO.NHENG-2492, 2025.

Froehlich, D. C.: Peak outflow from breached embankment dam, Journal of water Resources Planning and management, 121, 90-97, 1995.

GAPHAZ: Assessment of Glacier and Permafrost Hazards in Mountain Regions – Technical Guidance Document. , Zurich, Switzerland / Lima, Peru, , 72, 2017.

Huggel, C., Kääb, A., Haeberli, W., Teysseire, P., and Paul, F.: Remote sensing based assessment of hazards from glacier lake outbursts: a case study in the Swiss Alps, Canadian Geotechnical Journal, 39, 316-330, http://www.nrcresearchpress.com/doi/pdfplus/10.1139/t01-099, 2002.

Kapitsa, V., Shahgedanova, M., Machguth, H., Severskiy, I., and Medeu, A.: Assessment of evolution and risks of glacier lake outbursts in the Djungarskiy Alatau, Central Asia, using Landsat imagery and glacier bed topography modelling, Nat. Hazards Earth Syst. Sci., 17, 1837-1856, https://doi.org/10.5194/nhess-17-1837-2017, 2017.

Khanal, N. R., Hu, J.-M., and Mool, P.: Glacial lake outburst flood risk in the Poiqu/Bhote Koshi/Sun Koshi river basin in the Central Himalayas, Mountain Research and Development, 35, 351-364, http://www.bioone.org/doi/pdf/10.1659/MRD-JOURNAL-D-15-00009, 2015.

Lee, E., Carrivick, J. L., Quincey, D. J., Cook, S. J., James, W. H., and Brown, L. E.: Accelerated mass loss of Himalayan glaciers since the Little Ice Age, Scientific reports, 11, 24284, https://doi.org/10.1038/s41598-021-03805-8, 2021.

Popov, N.: Assessment of glacial debris flow hazard in the north Tien-Shan, Proceedings of the Soviet-China-Japan Symposium and field workshop on natural disasters, 384-391,

Rahman, M. M. and Bai, L.: Probabilistic seismic hazard assessment of Nepal using multiple seismic source models, Earth and Planetary Physics, 2, 327-341, 10.26464/epp2018030, 2018.

Sakai, A.: Glacial lakes in the Himalayas: a review on formation and expansion processes, Global Environmental Research, 16, 23-30, https://doi.org/10.57466/ger.16.1_23, 2012.

Singh, A., Shrestha, D., Ghimire, K., Mishra, S., Rana, D., and Acharya, S.: Assessing machine learning models to generate permafrost distribution map in Solukhumbu, Nepal, Geodesy and Geodynamics, 16, 275-287, https://doi.org/10.1016/j.geog.2024.08.003, 2025.

Wang, X., Liu, S., Ding, Y., Guo, W., Jiang, Z., Lin, J., and Han, Y.: An approach for estimating the breach probabilities of moraine-dammed lakes in the Chinese Himalayas using remote-sensing data, Natural Hazards and Earth System Sciences, 12, 3109-3122, https://doi.org/10.5194/nhess-12-3109-2012, 2012.

Zhang, G., Bolch, T., Yao, T., Rounce, D. R., Chen, W., Veh, G., King, O., Allen, S. K., Wang, M., and Wang, W.: Underestimated mass loss from lake-terminating glaciers in the greater Himalaya, Nature Geoscience, 1-6, https://doi.org/10.1038/s41561-023-01150-1, 2023a.

Zhang, T., Wang, W., and An, B.: A conceptual model for glacial lake bathymetric distribution, The Cryosphere, 17, 5137-5154, https://doi.org/10.5194/tc-17-5137-2023, 2023b.